J|A|C|S ARTICLES

Published on Web 11/30/2009

The Ni(II)-Binding Properties of the Metallochaperone SlyD

Harini Kaluarachchi,[†] Duncan E. K. Sutherland,[‡] Alex Young,[†] Ingrid J. Pickering,[§] Martin J. Stillman,[‡] and Deborah B. Zamble*,[†]

Department of Chemistry, University of Toronto, Toronto, Ontario, Canada M5S 3H6, Department of Chemistry, University of Western Ontario, London, Ontario, Canada N6A 5B7, and Department of Geological Sciences, University of Saskatchewan, Saskatoon, Saskatchewan, Canada S7N 5E2

Received September 25, 2009; E-mail: dzamble@chem.utoronto.ca

Abstract: Metallochaperones are essential for the safe and targeted delivery of necessary yet toxic metal cofactors to their respective protein partners. In this study we examine the nickel-binding properties of the *Escherichia coli* protein SlyD, a factor that contributes to optimal nickel accumulation in this organism. This protein is also required for *E. coli* energy metabolism because it participates in the nickel insertion step during [Ni−Fe]-hydrogenase metallocenter assembly. Our study demonstrates that SlyD is a multiple nickel ion binding protein. The analysis of noncovalent metal−protein complexes via electrospray ionization mass spectrometry revealed that SlyD binds up to seven nickel ions in a noncooperative manner with submicromolar affinity ($<2\ \mu$M, upper limit) and that the protein exists in a dynamic mixture of metalloforms that is dependent on the availability of nickel ions in solution. Structural analysis indicates that this metallochaperone undergoes small but distinct changes in the structure upon metal binding and that the nickel-binding sites are assembled through β-turn formation. Although the C-terminal metal-binding domain is primarily responsible for metal chelation, we find that metal binding also perturbs the structure of the N-terminal domains. An investigation of the nickel sites by using X-ray absorption spectroscopy shows that SlyD binds nickel ions by adapting several different geometries and coordination numbers. Finally, the characterization of SlyD mutants demonstrates that the cysteine residues in the C-terminal domain confer tighter affinity as well as increased binding capacity to SlyD. On the basis of the presented data a model for nickel binding to SlyD as well as its role in nickel homeostasis is discussed.

1. Introduction

Nickel plays a significant role in microorganisms, where the partnership between this metal and proteins is essential for a multitude of diverse biological functions.[1−3] Only present at nanomolar concentrations in the environment,[4,5] many organisms have evolved to utilize this transition metal ion in a variety of metalloenzymes such as urease, [NiFe]-hydrogenase, a superoxide dismutase, and acetyl-coenzyme A synthase.[1−3] Although essential, the limited availability and the inherently reactive nature of nickel ions create the necessity for strict control within the cellular milieu. Hence, the biogenesis of many of the intricate nickel-containing enzyme centers requires sets of proteins that include factors dedicated to the transport and delivery of the Ni(II) ions to the target proteins.[1,3] These soluble metal-trafficking proteins are referred to as metallochaperones.[6,7]

The [NiFe]-hydrogenases are crucial for energy metabolism in *Escherichia coli* where the enzymes catalyze the oxidation or production of hydrogen gas.[8,9] These bacteria express at least three isozymes of [NiFe]-hydrogenases that all have nickel- and iron-containing bimetallic centers at the active site.[10] Most of the pleitropic accessory proteins required for the multistep biosynthesis of these metallocenters are encoded by the *hyp* operon,[8,9,11] and the responsibilities of these proteins include delivery of both types of metal ions, synthesis of organic ligands, and protein folding. Although many of the mechanistic details are not yet known, HypA and HypB are thought to facilitate the Ni(II) insertion step of this pathway.[9,11] Furthermore, analysis of bacterial multiprotein complexes led to the discovery that HypB forms a complex with a protein called SlyD, which suggested that SlyD also participates in hydrogenase biosynthesis.[12] This hypothesis was supported by experiments with Δ*slyD* strains of *E. coli*, which exhibited reduced activity levels of all three [NiFe]-hydrogenases.[12] That this phenotype could be complemented by the addition of excess nickel to the media

[†] University of Toronto.
[‡] University of Western Ontario.
[§] University of Saskatchewan.

(1) Mulrooney, S. B.; Hausinger, R. P. *FEMS Microbiol. Rev.* **2003**, *27*, 239–261.
(2) Ragsdale, S. W. *J. Biol. Chem.* **2009**, *284*, 18571–18575.
(3) Li, Y.; Zamble, D. B. *Chem. Rev.* **2009**, *109*, 4617–43.
(4) Barceloux, D. G. *Clin. Toxicol.* **1999**, *37*, 239–258.
(5) Muyssen, B. T. A.; Brix, K. V.; DeForest, D. K.; Janssen, C. R. *Environ. Rev.* **2004**, *12*, 113–131.
(6) O'Halloran, T. V.; Culotta, V. C. *J. Biol. Chem.* **2000**, *275*, 25057–25060.
(7) Rosenzweig, A. C. *Chem. Biol.* **2002**, *9*, 673–677.
(8) Böck, A.; King, P. W.; Blokesch, M.; Posewitz, M. C. *Adv. Microb. Physiol.* **2006**, *51*, 1–71.
(9) Forzi, L.; Sawers, R. G. *Biometals* **2007**, *20*, 565–578.
(10) Vignais, P. M.; Billoud, B. *Chem. Rev.* **2007**, *107*, 4206–4272.
(11) Leach, M. R.; Zamble, D. B. *Curr. Opin. Chem. Biol.* **2007**, *11*, 159–165.
(12) Zhang, J. W.; Butland, G.; Greenblatt, J. F.; Emili, A.; Zamble, D. B. *J. Biol. Chem.* **2005**, *280*, 4360–4366.

10.1021/ja9081765

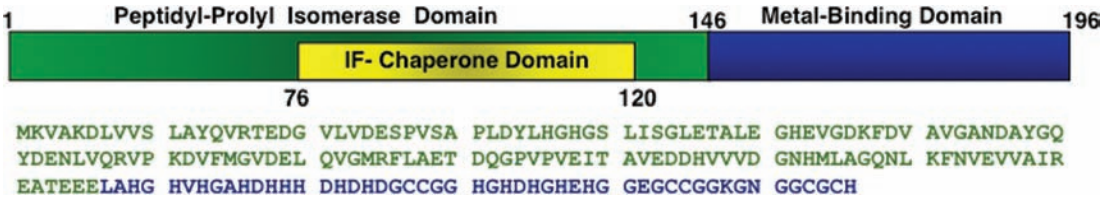

Figure 1. SlyD domain architecture and amino acid sequence. The amino acid sequence is color coded according to the domains. The PPIase domain is homologous to the FK506-binding proteins. The SlyD metal-binding domain is not conserved in all SlyD homologues, although many have sequences of variable length that are rich in potential metal-binding residues.

indicated that SlyD contributes specifically to the nickel-loading step of the hydrogenase metallocenter assembly pathway.[12]

Originally identified as a protein that sensitizes *E. coli* to lysis by bacteriophage ΦX174,[13] SlyD is a member of the FK506-binding protein (FKBP) family of peptidyl-prolyl isomerases (PPIase).[14,15] The PPIase domain located at the N-terminus of the protein (Figure 1) catalyzes the intrinsically slow interconversion of peptidyl-prolyl amide bonds, thereby assisting in protein folding.[16−18] In addition to the isomerase function, which is nonessential for hydrogenase biosynthesis,[19] SlyD also possesses general chaperone activity similar to that of many other FKBPs.[16,18] This latter property is attributed to an additional domain inserted within a loop of the PPIase domain termed IF (insertion in the flap) that is observed in a subset of FKBPs.[20,21] Deletion of several residues in the SlyD IF domain prevents interaction with HypB and abrogates SlyD's function in hydrogenase production in vivo.[22]

The last 50 amino acids of SlyD encompass an unusual domain that is rich in the potential metal-binding residues histidine, cysteine, aspartate, and glutamate. Given the composition of this domain, it is not surprising that SlyD is capable of coordinating a range of transition metal ions such as Co(II), Ni(II), and Cu(II), as well as Zn(II).[14,23] Several HypB homologues are also capable of binding multiple metal ions due to His-rich sequences, and in these organisms HypB is thought to contribute to nickel storage in addition to hydrogenase production.[24] The lack of such a region in *E. coli* HypB and the ability of SlyD to bind nickel ions led to the proposal that SlyD is responsible for nickel storage in *E. coli* and that it serves as a source of nickel for the production of the hydrogenase enzymes.[22,23] This hypothesis was supported by the observations that SlyD influences nickel accumulation in this organism and that the C-terminal domain of SlyD is required for the optimal production of hydrogenase activity.[22] SlyD also influences nickel release from a metal-binding site of HypB, suggesting another, more active task for SlyD during hydrogenase biosynthesis.[22]

The NMR solution structures of both a truncated version of *E. coli* SlyD (1−165) and the full-length protein were recently reported.[21,25] The structures reveal that the PPIase and IF domains of SlyD resemble those of other members of the FKBP family,[26] but in both cases the metal-binding regions were unstructured. To further understand the function of SlyD as a metallochaperone and its role in nickel homeostasis, a detailed characterization of nickel binding to SlyD is reported here. Our investigation revealed SlyD to be a monomeric protein containing multiple metal sites of similar affinities. Nickel binding occurs via a noncooperative mechanism, and the protein chelates nickel by using a mixture of coordination geometries. Through the study of a range of mutants we find that the cysteine residues in the C-terminal domain confer higher affinity as well as increased binding capacity to SlyD. Furthermore, although this domain is primarily responsible for metal binding to SlyD, the effects of metal binding are not limited to this domain in the protein.

2. Materials and Methods

2.1. Materials. Pfu DNA polymerase was purchased from Stratagene. Primers (Supporting Information, Table S1) were purchased from Sigma Genosys. All chromatography media were from GE Healthcare. Kanamycin, tris(2-carboxyethyl)phosphine (TCEP), dithiothreitol (DTT), isopro-β-D-1-galactopyranoside (IPTG) were purchased from BioShop (Toronto, ON). Metal salts were, as a minimum, 99.9% pure and purchased from Aldrich. The concentrations of the metal stock solutions were verified by ICP-AES. Several of the metal-binding studies were performed with atomic absorption standard solutions (AAS grade) where noted. Other reagents were analytical grade from Sigma. The buffers for all metal assays were treated with Chelex-100 (Bio-Rad) to minimize trace metal contamination. All samples were prepared with Milli-Q water, 18.2 MΩ-cm resistance (Millipore).

2.2. Generation of SlyD Mutants. Point mutations of SlyD were generated in the parent SlyD-pET24b vector[12] by using the QuickChange PCR mutagenesis method and *Pfu* polymerase along with forward and reverse primers listed in Table S1, Supporting Information. The resulting PCR plasmids were transformed into XL-2 Blue *E. coli* heat-shock competent cells (Stratagene) and isolated using Qiagen plasmid mini-prep kit. The pET24b-SlyD mutation constructs were verified by sequencing in the forward and reverse directions (ACGT, Toronto, ON). Three different mutants targeting each pair of cysteine residues were created and are as follows: SlyD C167,168A; SlyD C184,185A; and SlyD Δ193−196. A fourth mutant containing all of the above-mentioned mutations

(13) Roof, W. D.; Young, R. *J. Bacteriol.* **1993**, *175*, 3909–12.
(14) Wulfing, C.; Lombardero, J.; Pluckthun, A. *J. Biol. Chem.* **1994**, *269*, 2895–2901.
(15) Roof, W.; Horne, S.; Young, K.; Young, R. *J. Biol. Chem.* **1994**, *269*, 2902–2910.
(16) Kang, C. B.; Hong, Y.; Dhe-Paganon, S.; Yoon, H. S. *Neurosignals* **2008**, *16*, 318–25.
(17) Gothel, S. F.; Marahiel, M. A. *Cell. Mol. Life Sci.* **1999**, *55*, 423–436.
(18) Scholz, C.; Eckert, B.; Hagn, F.; Schaarschmidt, P.; Balbach, J.; Schmid, F. X. *Biochemistry* **2006**, *45*, 20–33.
(19) Zhang, J. W.; Leach, M. R.; Zamble, D. B. *J. Bacteriol.* **2007**, *189*, 7942–7944.
(20) Furutani, M.; Iida, T.; Yamano, S.; Kamino, K.; Maruyama, T. *J. Bacteriol.* **1998**, *180*, 388–394.
(21) Weininger, U.; Haupt, C.; Schweimer, K.; Graubner, W.; Kovermann, M.; Bruser, T.; Scholz, C.; Schaarschmidt, P.; Zoldak, G.; Schmid, F. X.; Balbach, J. *J. Mol. Biol.* **2009**, *387*, 295–305.
(22) Leach, M. R.; Zhang, J. W.; Zamble, D. B. *J. Biol. Chem.* **2007**, *282*, 16177–16186.
(23) Hottenrott, S.; Schumann, T.; Pluckthun, A.; Fischer, G.; Rahfeld, J. U. *J. Biol. Chem.* **1997**, *272*, 15697–15701.
(24) Kuchar, J.; Hausinger, R. P. *Chem. Rev.* **2004**, *104*, 509–526.
(25) Martino, L.; He, Y.; Hands-Taylor, K. L. D.; Valentine, E. R.; Kelly, G.; Giancoloa, C.; Conte, M. R. *FEBS J.* **2009**, *276*, 4529–4544.
(26) Suzuki, R.; Nagata, K.; Yumoto, F.; Kawakami, M.; Nemoto, N.; Furutani, M.; Adachi, K.; Maruyama, T.; Tanokura, M. *J. Mol. Biol.* **2003**, *328*, 1149–1160.

resulting in a protein devoid of any cysteines and referred to as the Triple mutant here onward, was also prepared.

2.3. Protein Expression and Purification. SlyD wild-type (WT) protein and mutants were expressed according to the method previously described[12] except that the mutants were expressed in a Δ*slyD* BL21(DE3) strain of *E. coli.*[22] SlyD and SlyD variants were purified by using a nickel-nitrilotriacetic acid (Ni-NTA, Qiagen) column followed by anion exchange on a MonoQ column (GE Healthcare). The presence of SlyD in the protein fractions collected at each step was verified by SDS-PAGE. After purification of the protein via the MonoQ column we noted that, for several fractions containing SlyD (with the exception of the Triple mutant), there was an unexpected absorption band at 320 nm that varied in intensity. ESI-MS analysis of the protein fractions that exhibited the 320 nm absorption did not resolve a mass difference (data not shown), the absorption was not affected by treatment with ethylenediaminetetraacetic acid (EDTA), and bound metal was not detected in metal analysis.[27] We also noted that by collecting only the fractions with $A_{320}/A_{280} < 0.1$ (i.e. fractions without the absorption at 320 nm) we are able to modify all the cysteine residues upon reaction with *N*-ethyl maleimide (NEM) (see below for reaction conditions). In contrast, the fractions with the absorption at 320 nm could not be completely modified by NEM and showed lower nickel-binding capacity in nickel titration experiments compared to the fully reduced protein fractions (data not shown). For these reasons, the absorption is assigned to an oxidation product of the Cys residues but the identity of this oxidation product is not yet known. Treatment with several reducing reagents (TCEP, dithionite, β-mercaptoethanol, DTT) has proven unsuccessful in reducing the Cys residues to the thiolate form while keeping the protein intact. Thus, only fractions without this absorption were pooled and further purified via gel-filtration on a Superdex S-75 column equilibrated with 20 mM HEPES, pH 7.5, 100 mM NaCl, 2 mM TCEP, and used in all the experiments described here. The purity of the final protein fractions were verified by ESI-MS, and the masses obtained are listed in Table S2, Supporting Information.

2.4. *N*-Ethyl Maleimide (NEM) Modification Assay. To prepare apoprotein, samples were pretreated with 4 mM TCEP and 20 mM EDTA overnight in an anaerobic glovebox at 4 °C. The protein was then gel filtered twice through PD-10 columns (GE Healthcare) equilibrated with 20 mM HEPES, pH 7.5, 100 mM NaCl (buffer A). An aliquot of this gel-filtered sample was reacted with a freshly prepared NEM solution in the same buffer. The final concentration of NEM in all reactions was approximately 5 times the concentration of cysteines in the protein ([NEM] = 5 × # of Cys × [protein]). The reaction samples were incubated overnight at 4 °C and were desalted prior to analysis by ESI-MS. Only protein samples that could be fully modified at all cysteines were used in further experiments.

2.5. Metal-Binding Experiments. Apoprotein was prepared as described above, and then incubated with the indicated amount of Ni(II) (AAS grade diluted into buffer A) overnight at 4 °C in an anaerobic glovebox. Nickel binding was monitored by using electronic absorption spectroscopy.

2.6. Circular Dichroism (CD) Spectroscopy. Protein samples were pretreated with EDTA and TCEP as described above and buffer exchanged into 10 mM ammonium acetate, pH 7.5, using microcentrifugal devices (MWCO of 10,000) (Pall nanosep centrifuge devices) in an anaerobic glovebox. SlyD samples (60 μM) were incubated with known amounts of $NiCl_2$ overnight at 4 °C. Samples were loaded into a 0.1 cm cuvette and capped to minimize exposure to air. The spectra were collected on a Jasco J-710 spectropolarimeter by scanning in the wavelength range of 205−320 nm at room temperature. The final spectra obtained are averages of five scans collected by using a scan speed of 20 nm/min.

2.7. Equilibrium Dialysis Experiments. Microchambers of DIALYZER (Harvard Apparatus, Inc.) were utilized for equilibrium dialysis experiments that were all conducted at 4 °C overnight. The protein chamber contained 250 μL of protein solution (40 μM) in buffer A with 1 mM TCEP, and the ligand chamber was filled with 250 μL of approximately 10-fold excess $NiCl_2$ in the same buffer. The amount of protein-bound nickel and free nickel were determined by a high-performance liquid chromatography (HPLC) method described previously.[27] For HPLC analysis, which was conducted in triplicate, >50 μg of protein was dried by centrifugation under vacuum, reconstituted with metal-free concentrated HCl (Seastar Chemicals), and hydrolyzed by incubation overnight at 95 °C. The sample was dried again to remove HCl and reconstituted in 80 μL of Milli-Q water. This sample was injected onto an IonPak CS5A column attached to a metal-free Dionex BioLC HPLC system followed by postcolumn mixing with 4-(2-pyridylazo)resorcinol (PAR) and detection at 530 nm. To determine free nickel concentration, an equivalent volume of sample from the ligand chamber was analyzed as described above.

2.8. Analytical Gel Filtration. Analytical gel filtration experiments were performed on a Superdex 75-HR column (GE Healthcare) at 4 °C with a flow rate of 0.5 mL/min and an injection volume of 100 μL. A protein concentration of 100 μM containing 2 mM TCEP was used in all gel-filtration experiments with the column equilibrated with buffer A, containing similar amounts of reducing agent. SlyD samples were incubated with the indicated amounts of $NiCl_2$ overnight at 4 °C prior to use, and the column buffer for these runs was supplemented with $NiCl_2$ concentrations similar to that of the protein sample. The apparent molar mass of the protein (M_r) was calculated from the eluting volume (V_e) using the equation $K_{av} = (V_e - V_o)/(V_t - V_o)$, where K_{av} is the partition coefficient, V_t is the total column volume and V_o is the void volume. The column was calibrated by injecting 100 μL of the LMW gel-filtration standards kit (GE Healthcare). Calibrations and the sample runs were conducted in triplicate to ensure reproducibility.

2.9. X-ray Absorption Spectroscopy (XAS) Sample Preparation. The purified protein solutions were pretreated with 2 mM TCEP and 10 mM EDTA overnight and were buffer exchanged into 20 mM HEPES, pH 7.5, 100 mM NaCl and 2 mM TCEP to remove the chelator and then concentrated by using an Amicon Ultra Centrifugal Filter Device (Millipore, MWCO = 3000 Da) to an approximate volume of 200 μL. All protein samples were placed on ice, and 0.8 equiv of Ni(II) (AAS grade diluted in buffer A) was added gradually in multiple small aliquots to suppress protein aggregation. Glycerol was then added to the protein solutions to give final concentrations of 20% (v/v). The final protein concentrations of the samples were approximately 1 mM, and these were subsequently frozen with liquid nitrogen and stored at −80 °C. For XAS data acquisition the samples were thawed, transferred to 2 mm path length (2 mm × 4 mm × 20 mm) Lucite sample cuvettes, and refrozen and were maintained at 10 K using an Oxford Instruments liquid helium flow cryostat. Analysis of holoprotein samples subjected to several freeze/thaw cycles by using electronic absorption spectroscopy did not reveal any changes in the absorption profiles, indicating that this process utilized during XAS sample handling did not lead to the loss of any metal−protein interactions.

2.10. XAS Data Collection. XAS data were collected with the SPEAR3 storage ring containing 100−200 mA at the Stanford Synchrotron Radiation Lightsource (SSRL Beamline 7-3 for mutant proteins, beamline 9-3 for wild-type SlyD). Experiments employed a Si(220) double crystal monochromator with an upstream Rh-coated collimating mirror which also provided harmonic rejection; beamline 9-3 additionally has a downstream focusing mirror. Incident and transmitted intensities were measured by using an ion chamber filled with nitrogen gas, and the spectrum of the sample was measured in fluorescence using a Canberra 30-element detector. For each sample 4−8 scans were accumulated, and the energy was calibrated by reference to the absorption of a nickel metal foil measured simultaneously with each scan, assuming a lowest-energy inflection point of 8331.6 eV for nickel foil.

(27) Atanassova, A.; Lam, R.; Zamble, D. B. *Anal. Biochem.* **2004**, *335*, 103–11.

2.11. XAS Data Analysis. XAS data reduction and analysis were performed using the EXAFSPAK suite programs (http://ssrl.slac.stanford.edu/exafspak.html), employing a Gaussian pre-edge function and a weighted polynomial spline with normalization correction to extract the EXAFS oscillations, $\chi(k)$. The EXAFS was quantitatively analyzed by curve-fitting $\chi(k)$ directly as described,[28] using ab initio theoretical phase and amplitude functions calculated using FEFF, version 8.4.[29] Phase-shifted Fourier transforms were calculated by using theoretical phase functions from the largest EXAFS component. Proximal atoms that could be fit as nitrogen or oxygen were fit as nitrogen. To fit EXAFS arising from histidine ligands coordinated to Ni(II), FEFF 8.25 was used to generate theoretical phase and amplitude parameters for full multiple scattering pathways containing second and third coordination sphere C and N atoms, using a model abstracted from the EXAFSPAK program mol-opt. All possible scattering pathways were included during fitting analysis, and no tilt or wag was introduced into the histidine orientation. The Debye−Waller factor of all of the multiple scattering pathways was varied at a fixed difference from that of the ligating nitrogen. For clarity, only the first shell Ni−$N_{imidazole}$ scattering pathway is listed Table S3, Supporting Information.

2.12. Sample Preparation and Instrument Conditions for ESI-MS. 2.12.1. Direct Ni(II) Titration of SlyD. Protein samples were pretreated with 10 mM EDTA and 2 mM TCEP for 24 h at 4 °C in an anaerobic glovebox. The samples were then gel-filtered via PD-10 columns using 10 mM ammonium acetate, pH 7.5. To minimize the sodium ion content in the sample the gel-filtered samples were subjected to further buffer exchanges into the same buffer via nanosep centrifugal devices MWCO 10000 (PALL Lifesciences). The metal solutions and the protein samples prepared under anaerobic conditions were septum capped to minimize oxidation of the protein prior to ESI-MS measurements. Direct Ni(II) titration results were obtained by injecting the protein sample with a known amount of Ni(II) acetate solution and allowing the sample to equilibrate for 3−4 min prior to acquiring the mass spectra. The mass spectra were acquired on a AB/Sciex QStarXL mass spectrometer equipped with an ion spray source in the positive ion mode. Ions were scanned from *m/z* 1200−3500 with accumulation of 1 s per spectrum with no interscan time delay and averaged for 35 cycles under MCA mode. The instrument parameters are as follows: ion source gas 50.0 psi; curtain gas 45.0 psi; ion spray voltage 5500.0 V; declustering potential 150.0 V; focusing potential 210 V; collision gas 3.0; MCP (detector) 2200.0 V. The nickel titration of $SlyD_{1-146}$ was conducted in a similar manner under aerobic conditions, and the ions were scanned in the *m/z* range of 650−2400 with an ion spray voltage set to 5300 V and a declustering potential of 50.0 V. The spectra were deconvoluted using the Bayesian protein reconstruction program over a mass range of 20000−22000 Da and 15000−17000 Da for SlyD WT and $SlyD_{1-146}$, respectively. A step mass of 1 Da, signal/noise ratio of 10, and the minimum intensity detected set to 1% was used during reconstruction of the data.

2.12.2. Titration of Nickel-Bound SlyD with Competitors (EGTA and Glycine). Fractions of the apoprotein in 10 mM ammonium acetate, pH 7.5, were incubated with excess nickel acetate overnight at 4 °C under anaerobic conditions. The protein sample was then gel filtered via a PD-10 column to remove excess metal. The collected holoprotein fractions were incubated with known amounts of the competitors, each prepared in chelexed Milli-Q water and adjusted to a pH of 7.5 by using ammonium hydroxide (metal-free grade). Samples were incubated 5 hrs at room temperature under an anaerobic environment prior to analysis via ESI-MS. The mass spectra were collected under identical instrument parameters as mentioned above except the ions were scanned in the *m/z* range of 1400−3500.

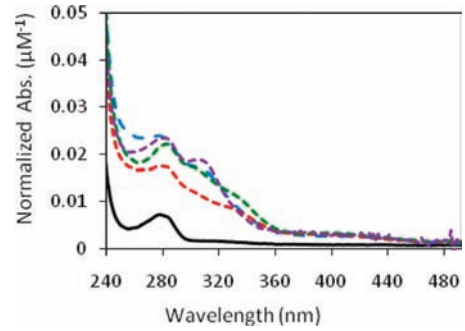

Figure 2. Electronic absorption spectra of wild-type SlyD and mutants. Upon incubation of SlyD (25 μM) with 7 mol equiv of nickel an absorption band is observed at 315 nm due to LMCT from sulfur to the Ni(II) center. The spectra of the mutants are different from that of WT suggesting alterations in the Ni(II) coordination environment as cysteines are replaced with alanines. Apo-WT (black solid line), holo-WT (blue dashed line), holo-SlyD C167,168A mutant (red dashed line), holo-SlyD C184,185A mutant (green dashed line), and holo-SlyD Δ193−196 (purple dashed line).

Table 1. Stoichiometry of Ni(II) Binding to SlyD

	average Ni(II) stoichiometry[a]	SD[b]
wild-type SlyD	4.2	0.2
SlyD C167,168A	2.6	0.2
SlyD C184,185A	2.8	0.4
SlyD Δ193−196	2.8	0.3
Triple mutant	1.9	0.4

[a] The averages reported are from three independent trials of equilibrium dialysis. [b] Standard deviation.

3. Results

3.1. Characterization of Ni(II) Binding to SlyD. The electronic absorption spectrum of SlyD incubated with Ni(II) revealed an absorption feature at 315 nm accompanied by an increase in the absorption at 280 nm (Figure 2). These bands are similar to the sulfur-to-metal charge transfer bands observed in the absorption spectra of small-molecule nickel-thiolate complexes[30,31] as well as other proteins that bind Ni(II) via Cys residues.[32−35] Titration of wild-type SlyD with nickel produced an increase in the absorption at 315 nm that saturated upon the addition of 4−5 equiv of metal, with the protein remaining soluble in solution even after the addition of a large excess of nickel ions (Figure S1, Supporting Information). It was unclear whether nickel was binding quantitatively to SlyD, so equilibrium dialysis experiments were conducted to obtain the stoichiometry of nickel binding to the protein. These experiments demonstrated that the protein coordinates 4.2 ± 0.2 Ni(II) ions/monomer (Table 1).

To determine whether nickel binding induces changes in the secondary structure of SlyD, CD spectroscopy was used. Two

(28) George, G. N.; Garrett, R. M.; Prince, R. C.; Rajagopalan, K. V. *J. Am. Chem. Soc.* **1996**, *118*, 8588–8592.
(29) Rehr, J. J.; Mustre de Leon, J.; Zabinsky, S. I.; Albers, R. C. *J. Am. Chem. Soc.* **1991**, *113*, 5135–5140.
(30) Ragunathan, K. G.; Bharadwaj, P. K. *J. Chem. Soc., Dalton Trans.* **1992**, 2417–2422.
(31) Rosenfield, S. G.; Berends, H. P.; Gelmini, L.; Stephan, D. W.; Mascharak, P. K. *Inorg. Chem.* **1987**, *26*, 2792–2797.
(32) Chivers, P. T.; Sauer, R. T. *Chem. Biol.* **2002**, *9*, 1141–1148.
(33) Iwig, J. S.; Leitch, S.; Herbst, R. W.; Maroney, M. J.; Chivers, P. T. *J. Am. Chem. Soc.* **2008**, *130*, 7592–7606.
(34) Leach, M. R.; Sandal, S.; Sun, H. W.; Zamble, D. B. *Biochemistry* **2005**, *44*, 12229–12238.
(35) Wang, S. C.; Dias, A. V.; Bloom, S. L.; Zamble, D. B. *Biochemistry* **2004**, *43*, 10018–10028.

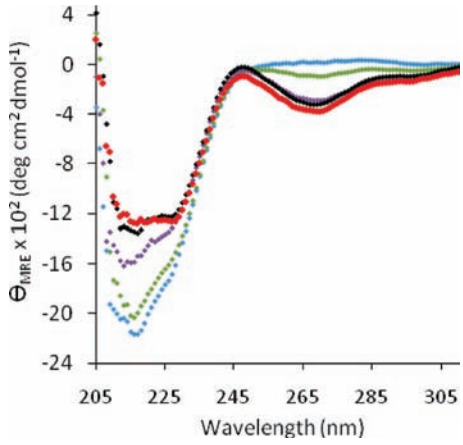

Figure 3. Ni(II)-induced secondary structural changes in SlyD. The intensity of the mean residue ellipticity in the far-UV decreases compared to that in the spectrum of the apoprotein (blue diamonds) as the protein is incubated with 1 equiv of Ni(II) (green diamonds), 2 equiv (purple diamonds), 4 equiv (black diamonds), and 8 equiv (red diamonds), suggesting the formation of β-turn type structure.

minima are observed in the spectrum of the apoprotein at 215 and 227 nm (Figure 3). The 215 nm absorption band signifies the existence of β-sheet structure in the protein, which is expected because of the predominance of β-sheets in both the PPIase and IF domains,[21,25] whereas the 227 nm band indicates a small amount of β-turn type structure.[23,36] As Ni(II) is titrated into the protein solution the molar ellipticity gradually decreases, in agreement with the trend that has been previously observed.[23] The changes in the CD signal, which reach a plateau upon addition of 4 mol equiv of Ni(II), are consistent with an increasing number of β-turns as SlyD chelates Ni(II) ions.[23,36] In addition, a near UV-CD band emerges at 270 nm as SlyD is incubated with nickel, with saturation reached at 2 equivalents of nickel. At this longer wavelength the likely chromophores are aromatic residues that are extremely sensitive to even minor structural perturbations due to events such as ligand binding, domain rearrangements, and protein−protein interactions.[37] Metal−protein complexes can also generate near UV−CD signals as a result of charge transfer between the metal ion and aromatic residues in the proteins, as observed in several cases.[38,39] Given that the aromatic residues in SlyD (tyrosine and phenylalanines) are exclusively located in the N-terminal PPIase and IF domains, these CD results suggest that the effects of nickel binding to SlyD are not limited to the metal-binding (MB) domain.

To investigate the quaternary structure of SlyD and the effects of Ni(II) on its oligomeric state, analytical gel filtration experiments were conducted (Figure S2, Supporting Information). Based on the partition coefficient an apparent molar mass ($M_{r,app}$) of 25 kDa was calculated for apo-SlyD. This mass is slightly higher than the theoretical molecular weight of 21 kDa, a mass that was confirmed by using ESI-MS (Table S2, Supporting Information). However, elution profiles corresponding to higher than the expected molecular masses have been observed for other histidine-rich proteins analyzed by size exclusion chromatography.[40,41] Hence, it can be concluded that SlyD exists as a monomeric protein at the concentrations (100 μM) used for analytical gel-filtration. Incubation of SlyD with 1 mol and 8 mol equiv of Ni(II) prior to gel filtration did not have a pronounced effect on the oligomeric state of SlyD (Figure S2, Supporting Information), resulting in only a slightly higher $M_{r,app}$ of 27 kDa and 28 kDa, respectively.

3.2. Analysis of Ni(II) Binding to SlyD by ESI-MS. To characterize the nickel-binding activity of SlyD in more detail, the protein was analyzed by ESI-MS as it was titrated with increasing amounts of nickel. This is the first report of utilizing ESI-MS to directly monitor the formation of nickel−protein complexes. The observed charge states and the corresponding deconvoluted spectra for a representative Ni(II) titration as well as a summary of the different species present at each titration point are shown in Figure 4. The data reveal the presence of several metalloforms that differ in nickel stoichiometries at each titration point, indicating that SlyD has multiple metal-binding sites with similar affinities for Ni(II). Furthermore, as in the case with the cysteine-rich metallothioneins,[42] the progressive detection of all of the possible metalated species signifies that Ni(II) binding to SlyD occurs via a noncooperative mechanism.

It has been established that the appearance of specific charge states is associated with the conformational status of a protein.[43] For metalloproteins, a change in the maximum and/or distribution of charge states can be associated with alterations in the size or conformation of the protein due to chemical changes such as metalation.[44,45] The *m*/*z* spectrum of apo-SlyD provides evidence for the presence of two different conformations of SlyD in solution (Figure 4). The fact that the relative peak intensities are higher for the smaller charge states suggests that the majority of the protein adopts a more folded conformation. The small population of lower *m*/*z* species observed in the spectrum of the apoprotein decreases in intensity upon Ni(II) addition, which clearly suggests that this population of SlyD adopts a more closed conformation upon Ni(II) binding. Thus, the MS data provide evidence for a Ni(II)-induced folding event, which is consistent with the Ni(II)-dependent structural changes observed via CD spectroscopy.

Upon analysis of the nickel titrations by MS a definitive end point could not be obtained before the concentration of salt interfered with the quality of the spectral data. Thus, a different approach was used to measure the stoichiometry of Ni(II) binding to SlyD. The protein was incubated with a 10-fold excess of metal overnight and then gel-filtered to remove any loosely bound Ni(II). The mass spectrum indicated the presence of a mixed population corresponding to a range of two to seven Ni(II) ions coordinated to the protein, with the dominant peaks arising from the four- and five-coordinated species (Figure 5). It is apparent from the MS data that holo-SlyD is a mixture of

(36) Perczel, A.; Hollosi, M. In *Circular Dichroism and the Conformational Analysis of Biomolecules*; Fasman, G. D., Ed.; Plenum Press: New York, 1996; pp 285−380.
(37) Woody, R. W.; Dunker, A. K. In *Circular Dichroism and the Confirmational Analysis of Biomolecules*; Fasman, G. D., Ed.; Plenum Press: New York, 1996; pp 109−158.
(38) Beltramini, M.; Bubacco, L.; Salvato, B.; Casella, L.; Gullotti, M.; Garofani, S. *Biochim. Biophys. Acta* **1992**, *1120*, 24–32.
(39) Vasak, M.; Kagi, J. H.; Holmquist, B.; Vallee, B. L. *Biochemistry* **1981**, *20*, 6659–64.
(40) Cun, S.; Li, H.; Ge, R.; Lin, M. C.; Sun, H. *J. Biol. Chem.* **2008**, *283*, 15142–51.
(41) Ge, R.; Watt, R. M.; Sun, X.; Tanner, J. A.; He, Q.-Y.; Huang, J.-D.; Sun, H. *Biochem. J.* **2006**, *393*, 285–293.
(42) Sutherland, D. E.; Stillman, M. J. *Biochem. Biophys. Res. Commun.* **2008**, *372*, 840–4.
(43) Kaltashov, I. A.; Abzalimov, R. R. *J. Am. Soc. Mass Spectrom.* **2008**, *19*, 1239–46.
(44) Rigby Duncan, K. E.; Kirby, C. W.; Stillman, M. J. *FEBS J.* **2008**, *275*, 2227–39.
(45) Pluym, M.; Vermeiren, C. L.; Mack, J.; Heinrichs, D. E.; Stillman, M. J. *Biochemistry* **2007**, *46*, 12777–87.

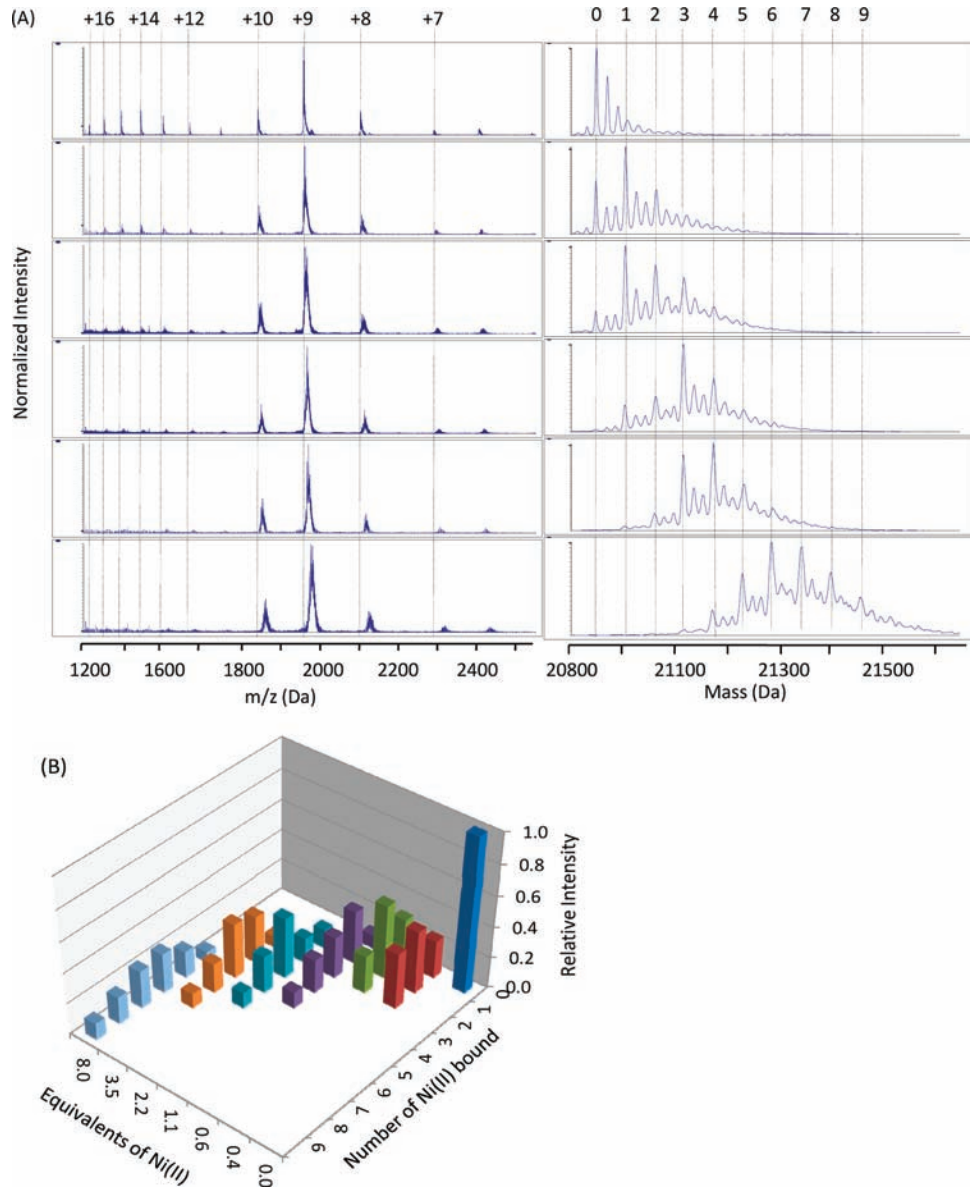

Figure 4. Analysis of Ni(II) binding to SlyD via ESI-MS. (A) Mass spectra recorded as increasing amounts of Ni(II) (0.0, 0.6 1.1, 2.2, 3.5, and 8 mol equiv, top to bottom) were added to apo-SlyD (34 μM). The associated deconvoluted spectra are shown on the right; the numbers above the peaks represent the number of nickel ions bound to each metalloform. (B) Graphical representation of the Ni(II) titration in which several metalloforms are observed at each titration point, indicating a noncooperative metal-binding mechanism. Note that the x-axis (Equivalents of Ni(II)) is not linear.

several metalloforms that exist concurrently, which likely leads to the average stoichiometry of 4.2 $\pm$ 0.2 obtained via equilibrium dialysis. This hypothesis is corroborated by the weighted sum of the metal-bound peaks observed in the MS that yields an average of 4.6 $\pm$ 0.1 nickel ions per SlyD.

To estimate the relative affinities of the multiple metal sites observed in the ESI-MS experiments, holo-SlyD was prepared by incubating apoprotein with excess nickel followed by gel filtration and then titration with increasing amounts of glycine prior to MS analysis. The number of metals bound to SlyD remained unaffected even in the presence of 128 mol equiv of the competitor, and the mass spectrum was almost identical to that of the protein in the absence of competitor (data not shown). Therefore, it can be deduced that the affinities of the detected metal sites are tighter than that of a Ni$-$(glycine)$_2$ complex ($K_a = 10^{5.74}$).[46] A similar experiment with EGTA, which is a competitor that forms a 1:1 complex with Ni(II) and has a higher affinity for the metal ($K_a = 10^{13.5}$),[46] was also conducted. The SlyD metal-binding sites were able to compete with EGTA (Figure S3, Supporting Information), although to a lesser extent than with glycine because an excess of EGTA could pull off almost all of the nickel from SlyD. Furthermore, the mass spectra recorded for the EGTA competition experiment provide evidence for the formation of a small population of ternary complex (approximately 1/6 of the intensity of the Ni-SlyD peaks, data not shown). The presence of the protein-Ni(II)-EGTA complex implies that metal release from SlyD does not solely rely on diffusion but that the chelator actively strips the metal from the protein via formation of a transient ternary complex. This observation also suggests that at least one of the metal sites is likely to be at the surface of the protein where it is accessible to the chelator.

3.3. X-ray Absorption Near-Edge Spectroscopy. To obtain structural information about the metal coordination environment in SlyD, WT protein loaded with 0.8 equiv of Ni(II) was analyzed by X-ray absorption spectroscopy (XAS). The absorp-

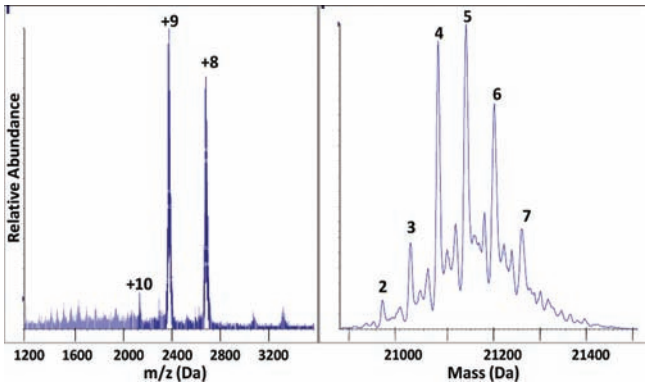

Figure 5. Stoichiometry of nickel binding to SlyD. Prior to analysis by ESI-MS, wild-type SlyD was incubated with a 10-fold molar excess of nickel overnight at 4 °C under anaerobic conditions (Left). The deconvoluted spectrum reveals 4−5 Ni(II) ion bound to SlyD as the predominant species present after gel filtration (right).

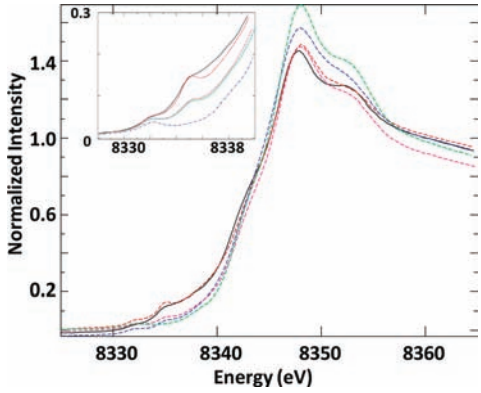

Figure 6. Ni K near-edge spectra. The overlaid spectra have been normalized to the edge jump. The samples include WT SlyD loaded with 0.8 equiv of Ni(II) (solid black line), as well as the mutants C167,168A (dashed red line), C184,185A (dashed green line), Δ193−196 (dashed purple line), and Triple mutant (dashed blue line) loaded with the same amount of metal.

tion edge around 8341 eV correlates well with the K-edge energy of previously analyzed Ni(II) complexes (Figure 6 and Figure S4, Supporting Information), and the general shape of the curve for the Ni(II) edge reflects a mixture of sites with either a square-pyramidal or octahedral environment as the major component.[47−50] The near-edge of SlyD exhibits two transitions of weak intensity, at 8332 and 8335 eV, as well as a shoulder at ~8342 eV. The small pre-edge feature at 8332 eV can be assigned to a 1s → 3d transition, and the peak area of this particular transition usually provides an indication of the geometry of the metal site. The 1s → 3d transition is formally dipole-forbidden but weakly quadrupole-allowed, and thus the expected intensity for this transition is minimal for rigorously centrosymmetric environments (i.e., square-planar or O_h). However, for noncentrosymmetic complexes (five-coordinate and T_d) the transition gains in intensity from dipole-allowed character due to increased p−d mixing.[47,51] The weak intensity in the SlyD spectrum suggests the presence of centrocymmetric complexes. The six and four-coordinate environments can usually be distinguished by a well-resolved peak at 8335 eV associated with the 1s → $4p_z$ transition (with shakedown contributions) of the latter complexes, and the weak peak at 8335 eV in the SlyD spectrum suggests a predominance of octahedral complexes with a minor amount of square-planar or distorted square-planar sites. The 1s → $4p_z$ transition is also observed in spectra of five-coordinate square-pyramidal complexes in the form of a shoulder-like feature at 8342 eV prior to the main edge peak,[47] as observed for SlyD. Furthermore, the height of the edge maximum is indicative of an environment with a significant number of O/N ligands.[52] Thus the XAS data clearly suggest the presence of multiple nickel sites with different geometries and coordination numbers. These data support the model in which nickel can bind to SlyD in several alternative sites with similar affinity.

3.4. Extended X-ray Absorption Fine Structure (EXAFS). Given that the near-edge data as well as the ESI-MS results indicate that even substoichiometric amounts of nickel bound to SlyD are distributed in several sites, obtaining an exact model of the nickel coordination environment from the EXAFS data of Ni(II)-WT SlyD may not be possible. Nevertheless the data were fit in an effort to provide qualitative information about the composition of the ligand sets. In order to minimize the number of variables, the mean coordination number of each type of ligand was systematically varied as integer values in each fit, although it is possible that the average number of a certain type of ligand around the different nickel sites may not be a whole number. Moreover, because the electronic absorption spectrum of wild-type SlyD indicates the presence one nickel−thiolate interaction, all fits included at least one cysteine ligand. Initial attempts to fit the data with only single-scattering pathways resulted in poor fits (selected fits are listed in Table S3, Supporting Information) and clearly did not model the intensity at 3−4 Å in the Fourier transform (FT) of the EXAFS data (Figure 7 and data not shown), which is due to atoms outside the primary coordination sphere of the Ni(II). This set of peaks is suggestive of one or more imidazole moieties chelating the Ni(II) ion,[51,53] and the distinct shoulder or "camel hump" feature observed in the EXAFS also supports histidine ligation of metal (Figure 7).[54,55] It is also possible that some of the signal in the 4 Å region is caused by a Ni(II)−Ni(II) interaction, which is feasible given that the ESI-MS demonstrates that the nickel can simultaneously fill several metal sites on the protein, but this possibility was not included in any fits.

The best fit of the wild-type SlyD EXAFS data was achieved with a five-ligand set including a single cysteine at 2.20 Å, two imidazoles with Ni−N distances of 2.08 Å, as well as two additional nitrogen or oxygen ligands at 2.16 Å (Table S3, Supporting Information, Fit 8, and Figure 7). The goodness of

(46) Martell, A. E.; Smith, R. M. National Institue of Standards and Technology: Rockville, MD, 2003.
(47) Colpas, G. J.; Maroney, M. J.; Bagyinka, C.; Kumar, M.; Willis, W. S.; Suib, S. L.; Baidya, N.; Mascharak, P. K. *Inorg. Chem.* **1991**, *30*, 920–928.
(48) Gu, W. W.; Jacquamet, L.; Patil, D. S.; Wang, H. X.; Evans, D. J.; Smith, M. C.; Millar, M.; Koch, S.; Eichhorn, D. M.; Latimer, M.; Cramer, S. P. *J. Inorg. Biochem.* **2003**, *93*, 41–51.
(49) Musgrave, K. B.; Laplaza, C. E.; Holm, R. H.; Hedman, B.; Hodgson, K. O. *J. Am. Chem. Soc.* **2002**, *124*, 3083–92.
(50) Tan, G. O.; Ensign, S. A.; Ciurli, S.; Scott, M. J.; Hedman, B.; Holm, R. H.; Ludden, P. W.; Korszun, Z. R.; Stephens, P. J.; Hodgson, K. O. *Proc. Natl. Acad. Sci. U.S.A.* **1992**, *89*, 4427–31.
(51) Davidson, G.; Clugston, S. L.; Honek, J. F.; Maroney, M. J. *Biochemistry* **2001**, *40*, 4569–4582.
(52) Haumann, M.; Porthun, A.; Buhrke, T.; Liebisch, P.; Meyer-Klaucke, W.; Friedrich, B.; Dau, H. *Biochemistry* **2003**, *42*, 11004–11015.
(53) Ferreira, G. C.; Franco, R.; Mangravita, A.; George, G. N. *Biochemistry* **2002**, *41*, 4809–18.
(54) Diakun, G. P.; Fairall, L.; Klug, A. *Nature* **1986**, *324*, 698–9.
(55) Stola, M.; Musiani, F.; Mangani, S.; Turano, P.; Safarov, N.; Zambelli, B.; Ciurli, S. *Biochemistry* **2006**, *45*, 6495–6509.

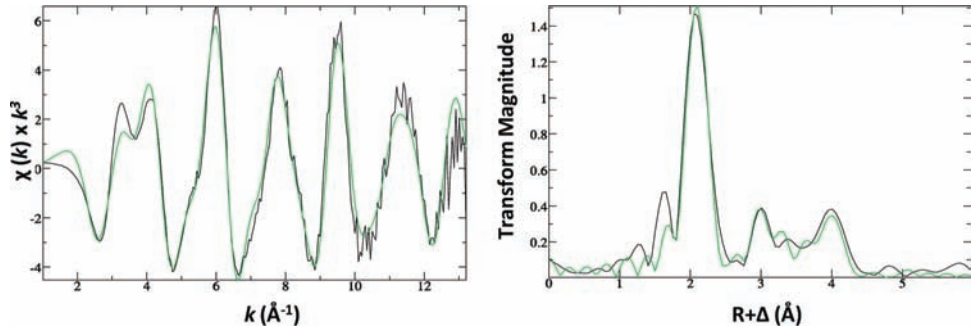

Figure 7. k^3-Weighted Ni(II) EXAFS data (left) and the Fourier transform of the data (right). Fourier transforms were phase corrected for the first shell interaction. The raw data for wild-type SlyD loaded with 0.8 equiv of Ni(II) is in black, and the best fit model (fit 8, 1S2N2His Table S3, Supporting Information) is in green.

fit, as indicated by the F-factor, did not change significantly upon fitting to three imidazoles, but visual inspection of the FT suggested that the histidine contribution was too high (data not shown). Reducing the number of histidines to one resulted in an increase in the F-factor, as did increasing the number of cysteines to two. Reasonable fits were also achieved with four and six ligand sets, but in both cases the best fits also included two imidazoles. The Ni−S distance of ≈ 2.2 Å that was observed in all of the best fits is in agreement with other 5-coordinate nickel compounds,[48] but it is also reasonable for four-coordinate complexes and has been observed in several nickel proteins with octahedral ligation.[48,52] Similarly, the Ni−N distances of the imidazole ligands (2.07−2.08 Å) are consistent with those of other nickel proteins.[56,57] The length of the additional bonds (>2.1 Å, either nitrogen or oxygen coordination) is unusually long, and some correlation between parameters increases the uncertainty of this distance in the fits. However, it is not atypical of nickel(II) complexes with cyclic ligands so it may indicate some constraints in the SlyD ligands,[58−60] or be a reflection of fitting a mixture of coordination environments.

3.5. Metal Chelation to the PPIase and IF Domains. The CD spectra of the nickel titration of WT SlyD suggested a metal-dependent structural perturbation in the N-terminal domains of the protein. These domains contain several potential metal-binding residues (Figure 1), so it is possible that the structural changes are independent of the metal-binding domain.[25] To test this possibility, a truncated variant of SlyD lacking the MB domain, $SlyD_{1-146}$, was analyzed by CD spectroscopy. The far-UV CD spectrum of $SlyD_{1-146}$ exhibits significantly more intense negative molar ellipticity, with a minimum at 208 nm and another transition at 222 nm (Figure S5, Supporting Information). These features may suggest a relatively higher degree of secondary structure, mainly α-helical, in comparison to the full-length protein. However, they could also be due to a decrease in structural elements such as β-turns and a partial opening up of the structure.[36,61] Regardless, it is clear that the metal-binding domain does have a significant effect on the overall structure of the protein even in the absence of metal. Incubation of $SlyD_{1-146}$ with increasing amounts of Ni(II) (up to 5 equiv, Figure S5, Supporting Information, and data not shown) did not change the CD spectrum at any wavelength measured, indicating that the metal-binding C-terminal domain is necessary to observe the structural changes in the N-terminal domains and suggesting that there is no direct nickel binding to the isolated N-terminal sections of the protein.

To test directly whether the N-terminal domains of SlyD have an independent metal-binding capacity, a Ni(II) titration of $SlyD_{1-146}$ was conducted in a manner similar to that for the WT protein and analyzed by using ESI-MS. As observed for the full-length protein, the MS spectrum of apo-$SlyD_{1-146}$ revealed that there are two populations of conformers differing in overall charge (data not shown). However, unlike the WT protein, the apo-$SlyD_{1-146}$ spectrum was dominated by lower *m*/*z* species, suggesting a more open conformation of the protein (data not shown), in agreement with the CD spectroscopy and confirming that the MB domain influences the overall structure of the protein. Furthermore, unlike the full-length protein, the population distribution did not change upon addition of nickel. Some nickel binding was observed in the MS, but a Ni(II)-bound protein peak was only detected upon addition of at least 2 mol equiv of Ni(II), and following incubation of the protein with 4 equiv of Ni(II) at least ∼30% of $SlyD_{1-146}$ still remained in the apo form. These results suggested that the Ni(II)−protein complexes detected via MS were a result of nonspecific interactions between the metal and the protein. To test this hypothesis, the protein sample was incubated with 8 mol equiv of Ni(II) overnight, then analyzed by MS following gel filtration. Only a peak corresponding to apo-$SlyD_{1-146}$ was detected in the gel-filtered samples, confirming that the metal−protein signals observed during the direct Ni(II) titration experiment arise from nonspecific, weak interactions with the N-terminal domains of SlyD.

3.6. Characterization of SlyD Mutants. To gain more insight into the involvement of the cysteine residues in metal binding, as suggested by the spectroscopic experiments, site-directed mutagenesis was employed. The six cysteines in SlyD are distributed throughout the metal-binding domain in pairs (Figure 1), so three mutants were generated in which each pair of Cys residues was either mutated to alanine (SlyD C167,168A and SlyD C184,185A) or removed (C193 and C195 are absent in the SlyD Δ193−196 truncation). Electronic absorption spectroscopy revealed that all three mutants bind Ni(II) (Figure 2), and titration experiments produced binding curves similar to that of the WT SlyD (data not shown). However, the electronic absorption signals of the mutants saturate with less nickel than

(56) Al-Mjeni, F.; Ju, T.; Pochapsky, T. C.; Maroney, M. J. *Biochemistry* **2002**, *41*, 6761–9.
(57) Colpas, G. J.; Brayman, T. G.; McCracken, J.; Pressler, M. A.; Babcock, G. T.; Ming, L.-J.; Colangelo, C. M.; Scott, R. A.; Hausinger, R. P. *J. Biol. Inorg. Chem.* **1998**, *3*, 150–160.
(58) Chandrasekhar, S.; McAuley, A. *J. Chem. Soc., Dalton Trans.* **1992**, 2967–2970.
(59) Goodman, D. C.; Reibenspies, J. H.; Goswami, N.; Jurisson, S.; Darensbourg, M. Y. *J. Am. Chem. Soc.* **1997**, *119*, 4955–4963.
(60) Halfen, J. A.; Young, V. G. J. *Chem. Commun.* **2003**, 2894–2895.
(61) Perczel, A.; Fasman, G. D. *Protein Sci.* **1992**, *1*, 378–395.

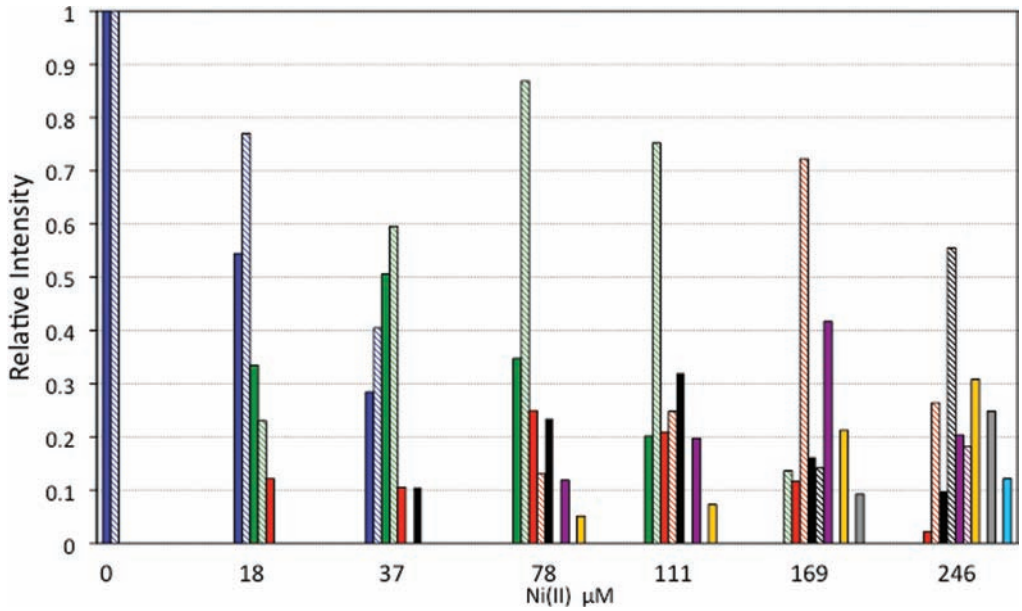

Figure 8. Competition for Ni(II) binding by WT and Triple mutant SlyD. An equimolar solution (25 μM each) of WT SlyD (solid bars) and Triple mutant (striped bars) was titrated with nickel in 10 mM ammonium acetate, pH 7.5. The relative intensity of different metalloforms at each titration point correlates to the relative abundance and is represented as follows: Apo (blue); 1, 2, 3, 4, 5, 6, and 7 Ni(II) ions bound: green, red, black, purple, yellow, gray, and light-blue bars, respectively.

wild-type SlyD, and the spectra from the mutants are altered. Less intense, slightly red-shifted LMCT bands are observed for the C167,168A and C184,185A mutants, whereas an increase in the intensity of the LMCT band is observed for the Δ193−196 protein (Figure 2). This preliminary analysis of the mutants implies changes in ligand environment and/or coordination geometry of the Ni(II) sites. The CD spectra of the apo- and holo- mutant proteins were similar to those of wild-type SlyD, indicating that mutations did not perturb the overall secondary structure of the protein (data not shown). Equilibrium dialysis experiments demonstrated that the nickel-binding capacity of all the mutants was reduced (Table 1), supporting a model in which all six Cys residues are involved in metal binding.

To determine if cysteines are necessary for any metal binding to SlyD, a fourth mutant was generated that lacked all six Cys residues by introducing all three of the sets of mutations mentioned above into *slyD* (referred to as the Triple mutant). As expected, no change was observed in the electronic absorption spectrum of the Triple mutant incubated with increasing amounts of Ni(II) (data not shown). However, the Triple mutant protein binds two Ni(II) per monomer in equilibrium dialysis experiments (Table 1). Given that the electronic absorption spectroscopy was performed with similar protein concentrations as the equilibrium dialysis experiments, the lack of a change in the absorption spectrum clearly denotes that the Ni(II) ions bind to donor atoms for which the LMCT is shifted well into the blue region of the spectrum. That the Triple mutant was chelating Ni(II) as a monomeric species was verified by analytical gel-filtration experiments (data not shown). MS analysis of the apo-Triple mutant indicated the presence of two different conformers with similar populations of *m*/*z* species as observed for the wild-type SlyD (data not shown). A Ni(II) titration revealed that the Triple mutant also adapts a more folded conformation when bound to nickel and that metal binding occurs via a noncooperative manner comparable to that of wild-type SlyD. However, in agreement with the equilibrium dialysis data the MS indicated reduced nickel-binding capacity for the Triple mutant.

To gain a better understanding of the importance of the thiolate ligands for metal binding, Ni(II) titrations of WT SlyD were performed in the presence of equimolar Triple mutant followed by ESI-MS analysis. Upon addition of 18 μM Ni(II) (~36% of the total protein concentration), peaks corresponding to 1 and 2 Ni(II) ions bound to WT appeared, whereas only a single bound ion was apparent for the Triple mutant (Figure 8), and less of WT was apoprotein in this competitive environment. In addition, the peak for apoprotein disappears at lower Ni(II) concentrations for the WT protein than for the mutant. No clear peaks could be distinguished in the mass spectrum past the 246 μM Ni(II) titration point for the WT SlyD due to interferences caused by the increased salt concentration. Nevertheless, wild-type SlyD clearly binds more nickel than the mutant, indicating that thiol moieties impart better metal-sequestering ability to SlyD but that the protein lacking cysteines is still competent at nickel binding.

3.7. XAS of SlyD Mutants. An overlay of the near-edge X-ray absorption spectra generated from WT SlyD and the mutant proteins provides clear evidence that the mutations alter the SlyD Ni(II)-binding sites (Figure 6). Although the overall shapes of the edge spectra are similar to those of WT, all the mutants exhibit an edge peak that is shifted to a higher energy. Furthermore, an increase in the intensity of the normalized fluorescence relative to the WT is also evident. These changes correlate well with the trend noted for Ni(II) complexes as S-donor ligands are substituted with N,O-donor ligands.[47] Very much like WT SlyD, the SlyD C167,168A and the SlyD Δ193−196 mutants' edge spectra exhibit features for a mixture of octahedral (8332 eV), square-pyramidal geometries (shoulder at 8342 eV) with some minor contributions from four-coordinate planar Ni(II) sites (8335 eV). The SlyD C184,185A mutant on the other hand appears to contain Ni(II) sites only in centrosymmetric geometries: octahedral and square planar. However, only a small fraction of this mutant forms the square-planar nickel sites since the intensity of the $1s \rightarrow 4p_z$ transition is very small. The spectrum of the Triple mutant produced the highest normalized intensity with a Ni(II) coordination environment that

is expected to solely contain oxygen and nitrogen donor ligands. The near-edge spectrum for this mutant contains a low intensity 1s → 3d transition at 8332 eV as well as a shoulder at 8342 eV corresponding to 1s → $4p_z$ transitions (which are suggestive of a mixture of metal sites with six-coordinate and square-pyramidal geometry) and lacks the peak at 8335 eV assigned to square-planar complexes. Therefore, the XAS data suggest the necessity of thiolate ligands to form low-coordination number, square-planar Ni(II) centers in SlyD. The FT of the EXAFS of the SlyD mutants loaded with nickel are similar to that of wild-type protein (Figure S6, Supporting Information), but the FT magnitude in the 3−4 Å region is larger for the Triple mutant compared to that of WT SlyD, suggesting that upon deletion of all Cys ligands the protein compensates with a larger number of histidine ligands in the coordination sphere.

4. Discussion and Conclusions

SlyD is an accessory protein required for achieving optimal levels of [NiFe]-hydrogenase activity in *Escherichia coli*.[12,22] Together with auxiliary proteins HypA and HypB, it is thought to act as a nickel chaperone that facilitates the Ni(II) insertion step in the maturation pathway of this enzyme,[11,12,22] and it may also serve as a nickel storage protein in this organism.[12] Of the three functional domains in SlyD, the PPIase domain, the molecular chaperone domain, and the C-terminal metal-binding domain, the latter two are essential for the role of SlyD in the enzyme biosynthetic pathway.[19,22] Although the molecular chaperone activity of SlyD has been investigated previously,[18,62] a detailed characterization of the nickel-binding properties has not been reported. Therefore, to obtain a better understanding of SlyD as a Ni(II)-binding protein and its function as a metallochaperone, nickel coordination to the protein was examined in detail by using a range of spectroscopic and spectrometric methods.

Consistent with the results from previous studies, we find that SlyD binds multiple metal ions but with a higher average nickel stoichiometry than previously noted.[14,23] The discrepancy in the data is likely due to the oxidation of the cysteine residues under atmospheric conditions, a hypothesis that is supported by the lower nickel-binding stoichiometries observed with the mutants in which cysteines were replaced with alanines (Table 1). Under physiological conditions SlyD should retain its full binding capacity given that the protein is located in the reducing cytosolic compartment and functions under anaerobic growth conditions, at least for its role in hydrogenase biosynthesis.[8] All of the experimental evidence supports the importance of the thiolate ligands for nickel binding. Not only do they impart higher nickel-binding capacity to SlyD, the Cys ligands enable the formation of metal sites with increased affinity for Ni(II). Although the amount of free nickel in the *E. coli* cytoplasm has not been measured, it is likely that it is a very competitive environment with the nickel ion distribution tightly controlled,[63−65] so the cysteine ligands would allow SlyD to sequester the potentially toxic nickel ions away from any weaker adventitious sites.

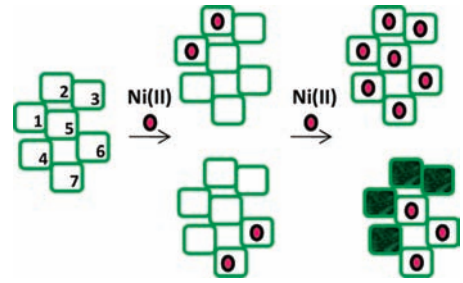

Figure 9. Model for Ni(II) binding to SlyD. The order of nickel binding to individual sites determines the maximum stoichiometry of the protein. For example, binding to sites 6 and 7 hinders the formation of sites 1−4 or inhibits access to these sites, whereas binding to sites 1 and 2 allows the protein to coordinate the metal to its full capacity, thereby leading to an equilibrium of several metalloforms.

Ni(II) ions fill the binding sites on SlyD in a progressive and overlapping fashion without altering the oligomeric state of the protein, indicating that metal binding is not cooperative. Although we anticipated preferential nickel binding to at least one higher-affinity site, the detailed electrospray mass spectrometry experiments show that SlyD exhibits multiple metal sites of similar affinity, and the X-ray absorption data reveal that even substoichiometric amounts of nickel produce a mixture of nickel coordination environments. Up to seven nickel ions remain bound to full-length SlyD following gel filtration chromatography and competition with glycine, indicating that all of the seven sites have at least low micromolar affinity for Ni(II) (K_D < 1.8 μM). The observation of nonspecific protein−metal complexes at high metal concentrations is an inherent issue of the ionization process utilized during positive mode metal−protein complex detection. However, the fact that the WT SlyD is able to chelate seven nickel ions even in the presence of glycine or the Triple mutant clearly indicates that all seven nickel ions are specifically bound by the protein. Furthermore, this is indicative that all seven metal sites may be utilized by the protein to bind nickel ions competitively in the bacterial cytosol. Although the MS data do not allow us to distinguish between nickel binding initially to one site and then redistribution to other sites versus concurrent filling of multiple sites, it does reveal the extreme plasticity of SlyD for metal binding and its ability to load a substantial amount of nickel ions. A similar metal coordination pattern has been observed for human metallothionein (MT-1), which exists in a dynamic mixture of metalloforms that is dependent on metal concentration in solution.[66−68]

That we were unable to achieve complete saturation via equilibrium dialysis at the maximal stoichiometry of seven bound nickel ions (that was observed in the MS) suggests that not all of the metal sites on SlyD are equally accessible. A possible explanation for this result can be derived from a model in which the metal-binding capacity of SlyD is governed by the sequence of Ni(II) binding to the seven metal sites (Figure 9). Given that all sites seem to be of similar affinity, binding to any of the sites would be equally probable initially. However, Ni(II) binding to a particular site (e.g., sites 6 and 7 instead of sites 1 and 2) may subsequently hinder the binding of Ni(II) to

(62) Knappe, T. A.; Eckert, B.; Schaarschmidt, P.; Scholz, C.; Schmid, F. X. *J. Mol. Biol.* **2007**, *368*, 1458–68.
(63) Bloom, S. B.; Zamble, D. B. *Biochemistry* **2004**, *43*, 10029–10038.
(64) Iwig, J. S.; Rowe, J. L.; Chivers, P. T. *Mol. Microbiol.* **2006**, *62*, 252–262.
(65) Rowe, J. L.; Starnes, G. L.; Chivers, P. T. *J. Bacteriol.* **2005**, *187*, 6317–6323.
(66) Salgado, M. T.; Bacher, K. L.; Stillman, M. J. *J. Biol. Inorg. Chem.* **2007**, *12*, 294–312.
(67) Rigby Duncan, K. E.; Stillman, M. J. *J. Inorg. Biochem.* **2006**, *100*, 2101–2107.
(68) Ngu, T. T.; Easton, A.; Stillman, M. J. *J. Am. Chem. Soc.* **2008**, *130*, 17016–17028.

other sites (i.e., 1−4) due to structural constraints imposed upon metal chelation, whereas binding to a different set of sites (i.e., sites 1 and 2) allows the protein to chelate the maximum number of nickel ions. The changes in conformation brought about by metalation along 'dead-end' pathways would be observed by very slow binding rates where complete metalation might not be realized within the hours of a typical experiment.[68] Kinetic experiments will be required to test this hypothesis.

Competition experiments with EGTA provide additional evidence for the similar affinity of the metal sites because the selective depletion of individual metalloforms (resulting in populations with only 4 Ni(II) ions bound to SlyD, for example) is not observed at any concentration of the competitor. These experiments also support the conclusion that the protein is able to chelate nickel in a competing cellular environment, which would be essential for its function as a source of nickel for hydrogenase biosynthesis under nickel-limiting conditions. The equilibrium dissociation constant of nickel binding to SlyD has an upper limit of low micromolar, placing it in a range that is similar to or tighter than that of nickel-binding proteins from other organisms such as Hpn, Hpn-like, or HspA from *Helicobacter pylori*,[40,41,69] UreE,[55,70] and histidine-rich HypB homologues.[71,72] This latter comparison, coupled with the fact that SlyD forms a complex with *E. coli* HypB, supports the hypothesis that one of the purposes of SlyD is to fill the role occupied by histidine-rich versions of HypB in other systems.

The CD spectroscopy, together with charge state distributions detected during the mass spectrometry experiments, is indicative of a protein capable of metal binding with small but distinctive changes in protein structure. The CD suggests that the changes induced by nickel binding are dominated by the formation of β-turn type structures that are localized to the C-terminal domain of the protein. A similar metal-induced structure formation has been previously observed for other proteins.[67,73,74] An analysis of a collection of proteins indicates that β-turns predominantly consist of hydrophilic amino acid residues and are concentrated at the protein surface.[36] Thus, it is likely that the metal-binding domain is located at the surface of the protein, an optimal position for facile nickel binding, and a position supported by the unstructured nature of this region in apo-SlyD.[21,25] Furthermore, in such a location the nickel ions could be tightly bound but not completely buried, allowing for direct transfer of nickel ions between SlyD and other proteins via ligand exchange reactions that would not entail a substantial conformational rearrangement in SlyD.

Considering the properties of SlyD, including a chaperone domain that enables protein−protein complex formation and an accessible metal-binding domain at the surface, it is evident that SlyD could participate in hydrogenase biosynthesis in one or more capacities.[11,12,22] The fact that it can bind many nickel ions suggests that SlyD functions as a store of nickel, which could be made available specifically to the hydrogenase pathway through complex formation with other accessory proteins such as HypB. HypB has an N-terminal metal-binding site with subpicomolar affinity for nickel;[34] thus, from a thermodynamic perspective it is feasible that it could abstract nickel from SlyD via a ternary complex such as that observed in the competition experiments with EGTA. However, HypB is not the final destination of the nickel ion in this pathway, and in vitro experiments demonstrate that SlyD increases the release of HypB-bound nickel to a third chelator,[22] so an alternative possibility is that SlyD helps to make this nickel available. The route of the nickel ion on its way to the hydrogenase precursor protein and whether other components of the nickel-insertion complex participate in nickel delivery are issues that remain to be defined by future experiments.

Unlike the full-length protein, any adventitious nickel ions bound to $SlyD_{1-146}$ were completely stripped away by gel filtration chromatography. The conclusion that the isolated PPIase domain does not chelate Ni(II) is supported by the CD experiments demonstrating that its structure is unaffected by the presence of Ni(II) in solution. Thus, the MB domain is required for tight nickel binding to SlyD. Although the metals bind to the C-terminus of SlyD, the N-terminal domains are also perturbed by this activity, as is evident from the appearance of the near-UV CD band upon nickel titration of the full-length protein. This perturbation could either result from metal binding to one or more sites that bridge the MB and the N-terminal domains, or from nickel binding to the MB domain producing an allosteric effect that propagates into the N-terminus. Experiments with the isolated MB domain designed to resolve this issue have been precluded to date due to excessive degradation. These conformational changes observed upon nickel binding may cause the nickel-induced inhibition of the PPIase activity that has previously been reported,[23] an effect not observed in the absence of the metal-binding domain. This connection is in agreement with a recent NMR study that revealed that the addition of nickel perturbs residues around the catalytic pocket of the PPIase domain.[25]

The fact that nickel binding to SlyD functions as a reversible switch that regulates the PPIase provides a link between the two activities of the protein. However, as with many PPIase enzymes,[17] it is not known whether this activity of SlyD has a cellular function, and thus the physiological relevance of this connection is unclear. The PPIase activity would only be blocked under anaerobic growth conditions because nickel import by *E. coli* is activated in the absence of oxygen,[75] the environmental conditions that also necessitate hydrogenase activity.[8] The PPIase activity of SlyD is not critical for hydrogenase biosynthesis,[19] but it has been proposed that it may be detrimental[25] and nickel binding could be a mechanism of preventing SlyD from catalyzing undesired isomerizations of prolines in the other hydrogenase accessory proteins or the enzyme itself. A similar metal-dependent switch mechanism has been observed for another bacterial heat-shock chaperone protein Hsp33.[76] Hsp33 normally exists in a deactivated form where Cys residues in the protein are coordinated to a zinc ion. When the bacteria undergo oxidative stress, the zinc ion is displaced, and the protein exhibits folding chaperone activity in its apo-form upon

(69) Zeng, Y. B.; Zhang, D. M.; Li, H.; Sun, H. *J. Biol. Inorg. Chem.* **2008**, *13*, 1121–1131.
(70) Lee, M. H.; Pankratz, H. S.; Wang, S.; Scott, R. A.; Finnegan, M. G.; Johnson, M. K.; Ippolito, J. A.; Christianson, D. W.; Hausinger, R. P. *Protein Sci.* **1993**, *2*, 1042–1052.
(71) Fu, C.; Olson, J. W.; Maier, R. J. *Proc. Natl. Acad. Sci. U.S.A.* **1995**, *92*, 2333–2337.
(72) Rey, L.; Imperial, J.; Palacios, J. M.; Ruiz-Argueso, T. *J. Bacteriol.* **1994**, *176*, 6066–6073.
(73) Yang, S.; Thackray, A. M.; Fitzmaurice, T. J.; Bujdoso, R. *Biochim. Biophys. Acta* **2008**, *1784*, 683–692.
(74) Munoz, A.; Dughish, M.; Specher, T.; Shaw, C. F.; Petering, D. H. *J. Inorg. Biochem.* **1999**, *74*, 302–302.
(75) Wu, L.-F.; Mandrand-Berthelot, M.-A.; Waugh, R.; Edmonds, C. J.; Holt, S. E.; Boxer, D. H. *Mol. Microbiol.* **1989**, *3*, 1709–1718.
(76) Jakob, U.; Muse, W.; Eser, M.; Bardwell, J. C. A. *Cell* **1999**, *96*, 341–352.

forming an oxidized dimer.[76,77] Whether SlyD is modulated by such a metal-dependent switch, in which it functions as a general protein-folding enzyme under aerobic conditions and switches to the more specific task of a Ni(II) chaperone for hydrogenase biosynthesis under anaerobic expression, has yet to be determined.

It is not uncommon for a chaperone protein to perform cellular functions in addition to its protein folding activity, and these extra functions are usually integrated into the chaperone in the form of an extra domain. For instance, the heat shock protein A (HspA) in *H. pylori* contains a metal-binding domain at the C-terminus that is beneficial for Ni(II) resistance in this organism.[40] Calreticulin is a chaperone involved in glycoprotein folding that also participates in the regulation of intracellular Ca(II) homeostasis.[78] In the case of the aforementioned Hsp33, incorporation of an oxygen-sensitive metal-binding domain at the C-terminus allows this protein to function as a chaperone in response to oxidative stress.[77] Augmentation of a constitutively expressed chaperone such as SlyD[15] with a metal-binding domain would be advantageous because a readily available sink for Ni(II) would be present when the bacteria switch to anaerobic metabolism and start importing nickel. In this manner, the cell would be protected from the toxic properties of this element while ensuring that the nickel is directed to where it is needed in the hydrogenase biosynthetic pathway.

SlyD homologues have been annotated in a large number of prokaryotic genomes,[79] and although the C-terminal domains are not well-conserved, many of the homologues have significant extensions rich in metal-binding residues. Thus, SlyD may be a key player in prokaryotic nickel homeostasis. For example, both biochemical and genetic experiments have implicated SlyD in the biosynthetic pathway for urease in the human pathogen *H. pylori*.[80,81] In view of the role of SlyD in nickel homeostasis in *E. coli*, the noncooperative, adaptable metal-binding nature of SlyD is analogous to metallothioneins that are proposed to be involved in the homeostasis of zinc levels in the human brain.[82,83] Although SlyD has been characterized in the context of a nickel-binding protein, there are several questions that remain to be resolved. With its high content of potential metal-binding residues can the protein function as a general metal detoxifier similar to metallothioneins? What is the metal-specificity of SlyD, and how does this specificity correlate with optimal biogenesis of the hydrogenase enzyme? Is it possible for SlyD to function as a metallochaperone for other enzymes? Additional work is underway to address these questions.

Acknowledgment. This work was supported in part by funding from the Natural Sciences and Engineering Research Council (Canada) and the Canada Research Chairs program. We thank Dr. G. Butland and Prof. A. Emili (University of Toronto), for the Δ*slyD* BL21(*DE3*) strains, and members of the Zamble laboratory, for helpful discussions. In particular, we thank Kathleen Zhang and Alistair Dias for preparation and data collection of the WT SlyD XAS sample and the Pickering and George group lab members for their help in XAS data collection. Portions of this research were carried out at the Stanford Synchrotron Radiation Lightsource, a national user facility operated by Stanford University on behalf of the U.S. Department of Energy, Office of Basic Energy Sciences. The SSRL Structural Molecular Biology Program is supported by the Department of Energy, Office of Biological and Environmental Research, and by the National Institutes of Health, National Center for Research Resources, Biomedical Technology Program.

Supporting Information Available: Tables S1−S3 containing PCR primer sequences, masses of SlyD and its variants verified by ESI-MS, and EXAFS curve fitting analysis of wild-type SlyD; Figures S1−S4 showing direct Ni(II) titration curve for SlyD WT, analytical gel-filtration results, graphical representation of the ESI-MS data for Ni(II)-SlyD titration with EGTA, and near-edge comparison of Ni(II)-SlyD to model complexes, respectively. Figure S5, comparison of CD spectra of WT vs $SlyD_{1-146}$; Figure F6, WT EXAFS curves and FT data overlaid with SlyD mutants.This material is available free of charge via the Internet at http://pubs.acs.org.

JA9081765

(77) Won, H. S.; Low, L. Y.; De Guzman, R.; Martinez-Yamout, M.; Jakob, U.; Dyson, H. J. *J. Mol. Biol.* **2004**, *341*, 893–899.
(78) Martin, V.; Groenendyk, J.; Steiner, S. S.; Guo, L.; Dabrowska, M.; Parker, J. M. R.; Muller-Esterl, W.; Opas, M.; Michalak, M. *J. Biol. Chem.* **2006**, *281*, 2338–2346.
(79) Erdmann, F.; Fischer, G. In *Metal Ions in Life Sciences*; Sigel, A., Sigel, H., Sigel, R. K. O., Eds.; John Wiley and Sons: New York, 2007; Vol. 2, pp 501−518.
(80) Benanti, E. L.; Chivers, P. T. *J. Bacteriol.* **2009**, *191*, 2405–8.
(81) Stingl, K.; Schauer, K.; Ecobichon, C.; Labigne, A.; Lenormand, P.; Rousselle, J.-C.; Namane, A.; De Reuse, H. *Mol. Cell. Proteomics* **2008**, *7*, 2429–2441.
(82) Palumaa, P.; Eriste, E.; Njunkova, O.; Pokras, L.; Jornvall, H.; Sillard, R. *Biochemistry* **2002**, *41*, 6158–6163.
(83) Palumaa, P.; Tammiste, I.; Kruusel, K.; Kangur, L.; Jornvall, H.; Sillard, R. *Biochim. Biophys. Acta* **2005**, *1747*, 205–211.